

Unified Treatment of Dynamical Processes on Generalized Networks: Higher-Order, Multilayer, and Temporal Interactions

Yuanzhao Zhang,^{1,2} Vito Latora,^{3,4,5,6} and Adilson E. Motter^{1,7}

¹*Department of Physics and Astronomy, Northwestern University, Evanston, Illinois 60208, USA*

²*Center for Applied Mathematics, Cornell University, Ithaca, New York 14853, USA*

³*School of Mathematical Sciences, Queen Mary University of London, London E1 4NS, United Kingdom*

⁴*Dipartimento di Fisica ed Astronomia, Università di Catania and INFN, I-95123 Catania, Italy*

⁵*The Alan Turing Institute, The British Library, London NW1 2DB, United Kingdom*

⁶*Complexity Science Hub Vienna (CSHV), Vienna, Austria*

⁷*Northwestern Institute on Complex Systems, Northwestern University, Evanston, Illinois 60208, USA*

When describing complex interconnected systems, one often has to go beyond the traditional network description to account for generalized interactions. Here, we establish a unified framework to optimally simplify the analysis of cluster synchronization patterns for a wide range of generalized networks, including hypergraphs, multilayer networks, and temporal networks. The framework is based on finding the finest simultaneous block diagonalization (SBD) of the matrices encoding the synchronization pattern and the interaction pattern. As an application, we use the SBD framework to characterize chimera states induced by nonpairwise interactions and by time-varying interactions. The unified framework established here can be extended to other dynamical processes and can facilitate the discovery of novel emergent phenomena in complex systems with generalized interactions.

Over the past two decades, networks have emerged as a versatile description of interconnected complex systems [1, 2]. However, it has also become increasingly clear that the original formulation of a static network representing a single type of pairwise interaction has its limitations. For this reason, the original formulation has been generalized in different directions, including hypergraphs [3], multilayer networks [4, 5], and temporal networks [6]. Naturally, with the increased descriptive power comes an increased analytical complexity, especially for dynamical processes on these generalized networks.

One important class of dynamical processes on networks is cluster synchronization. Many biological and technological networks show intricate cluster synchronization patterns, where one or more internally coherent but mutually independent clusters coexist [7–13]. Maintaining the desired dynamical patterns is critical to the function of those networked systems [14, 15]. For instance, long-range synchronization in the theta frequency band between the prefrontal cortex and the temporal cortex has been shown to improve working memory in older adults [16].

In this Letter, we develop a versatile framework that enables the stability analysis of synchronization patterns on generalized networks. Here, generalized networks include *hypergraphs* that account for nonpairwise interactions involving three or more nodes simultaneously, *multilayer networks* that accommodate mixed types of interactions (in different layers), and *temporal networks* whose connections change over time. The method we propose is based on establishing the finest simultaneous block diagonalization (SBD), which optimally decouples the variational equation and enables the exploration of complex synchronization patterns in large networks. We demonstrate the strength of our framework by studying chimera

states (an important class of cluster synchronization patterns) on hypergraphs and temporal networks.

General formulation and the SBD approach.— Consider a general set of equations describing N interacting oscillators:

$$\mathbf{x}_i[t+1] = \mathbf{F}(\mathbf{x}_i[t]) + \mathbf{h}_i(\mathbf{x}_1[t], \dots, \mathbf{x}_N[t], t), \quad (1)$$

where \mathbf{F} describes the intrinsic node dynamics and \mathbf{h}_i specifies the influence of other nodes on node i . We present our framework assuming discrete-time dynamics, although it works equally well for systems with continuous-time dynamics.

For a static network with a single type of pairwise interaction, $\mathbf{h}_i(\mathbf{x}_1, \dots, \mathbf{x}_N, t) = \sigma \sum_{j=1}^N C_{ij} \mathbf{H}(\mathbf{x}_i, \mathbf{x}_j)$, where σ is the coupling strength, the coupling matrix \mathbf{C} reflects the network structure, and \mathbf{H} is the interaction function. When the network is globally synchronized, $\mathbf{x}_1 = \dots = \mathbf{x}_N = \mathbf{s}$, the synchronization stability can be determined through the Lyapunov exponents associated with the variational equation:

$$\delta[t+1] = (\mathbf{I}_N \otimes \mathbf{J}\mathbf{F}(\mathbf{s}) + \sigma \mathbf{C} \otimes \mathbf{J}\mathbf{H}(\mathbf{s})) \delta[t], \quad (2)$$

where $\delta = (\mathbf{x}_1 - \mathbf{s}; \dots; \mathbf{x}_N - \mathbf{s})$ is the perturbation vector, \mathbf{I}_N is the identity matrix, \otimes represents the Kronecker product, and \mathbf{J} is the Jacobian operator. In this case of undirected networks, Eq. (2) can always be decoupled into N independent low-dimensional equations by switching to coordinates that diagonalize the coupling matrix \mathbf{C} [17].

For more complex synchronization patterns, however, additional matrices encoding information about dynamical clusters are inevitably introduced into the variational equation. In particular, the identity matrix \mathbf{I}_N is re-

placed by diagonal matrices $\mathbf{D}^{(m)}$ defined by

$$D_{ii}^{(m)} = \begin{cases} 1 & \text{if node } i \in \mathcal{C}_m, \\ 0 & \text{otherwise,} \end{cases} \quad (3)$$

where \mathcal{C}_m represents the m th dynamical cluster. Moreover, as we show below, when $\mathbf{h}_i(\cdot)$ includes nonpairwise interactions, multilayer interactions, or time-varying interactions, it leads to additional coupling matrices $\mathbf{C}^{(k)}$ and interaction functions $\mathbf{H}^{(k)}$ in the variational equation. Thus, the variational equations for complex synchronization patterns on generalized networks share the following form:

$$\delta[t+1] = \left\{ \sum_m \mathbf{D}^{(m)} \otimes \mathbf{JF}(\mathbf{s}^m) + \sum_{m,k} \sigma_k \mathbf{C}^{(k)} \mathbf{D}^{(m)} \otimes \mathbf{JH}^{(k)}(\mathbf{s}^m, t) \right\} \delta[t], \quad (4)$$

where \mathbf{s}^m is the synchronized state of the oscillators in the m th dynamical cluster.

For Eq. (4), diagonalizing any one of the matrices $\mathbf{D}^{(m)}$ or $\mathbf{C}^{(k)}$ generally does not lead to optimal decoupling of the equation. Instead, all of $\{\mathbf{D}^{(m)}\}$ and $\{\mathbf{C}^{(k)}\}$ should be considered concurrently and be simultaneously *block* diagonalized to reveal independent perturbation modes. In particular, the new coordinates should separate the perturbation modes parallel and transverse to the cluster synchronization manifold, and decouple transverse perturbations to the fullest extent possible.

For this purpose, we develop an algorithm to find an orthogonal transformation matrix \mathbf{P} that reveals the *finest* SBD of any given set of symmetric matrices. Given a set of symmetric matrices $\mathcal{B} = \{\mathbf{B}^{(1)}, \mathbf{B}^{(2)}, \dots, \mathbf{B}^{(\mathcal{L})}\}$, our SBD algorithm consists of three simple steps:

i) Find the (orthogonal) eigenvectors \mathbf{v}_i of the matrix $\mathbf{B} = \sum_{\ell=1}^{\mathcal{L}} \xi_{\ell} \mathbf{B}^{(\ell)}$, where ξ_{ℓ} are independent random numbers drawn from a Gaussian distribution. Set $\mathbf{Q} = [\mathbf{v}_1, \dots, \mathbf{v}_N]$.

ii) Generate $\mathbf{B} = \sum_{\ell=1}^{\mathcal{L}} \xi_{\ell} \mathbf{B}^{(\ell)}$ for a new realization of ξ_{ℓ} and compute $\tilde{\mathbf{B}} = \mathbf{Q}^{\dagger} \mathbf{B} \mathbf{Q}$. Mark the indexes i and j as being in the same block if $\tilde{B}_{ij} \neq 0$ (and thus $\tilde{B}_{ji} \neq 0$).

iii) Set $\mathbf{P} = [\mathbf{v}_{\epsilon(1)}, \dots, \mathbf{v}_{\epsilon(N)}]$, where ϵ is a permutation of $1, \dots, N$ such that indexes in the same block are sorted consecutively.

Intuitively, the above algorithm works because a random combination of $\mathbf{B}^{(\ell)}$ contains all the information about their common block structure (with probability 1), which can be efficiently extracted through eigendecomposition (see Supplemental Material [18] for a proof of the optimality of the discovered common block structure). In addition to establishing a unified framework for generalized networks, our SBD algorithm is also faster than any of its precedents: it scales with $\mathcal{O}(N^3)$ instead of $\mathcal{O}(N^4)$ [19–22] or $\mathcal{O}(\mathcal{L}N^3)$ [23]. Our algorithm can process matrices with $N \approx 1000$ in under a second (tested on an

Intel Xeon E5-2680 v3 Processor). Moreover, the algorithm requires the eigendecomposition of a single matrix, so its performance does not depend strongly on the number of matrices to be simultaneously block diagonalized. The MATLAB and Python implementations of our SBD algorithm are available online as part of this publication [24].

Cluster synchronization and chimera states on hypergraphs.— Hypergraphs [25] and simplicial complexes [26] provide a general description of networks with nonpairwise interactions and have been widely adopted in the literature [27–36]. However, the associated tensors describing those higher-order structures are more involved than matrices, especially when combined with the analysis of dynamical processes [37–42]. There have been several efforts to generalize the master stability function (MSF) formalism [17] to these settings, for which different variants of an aggregated Laplacian have been proposed [43–46]. The aggregated Laplacian captures interactions of all orders in a single matrix, whose spectral decomposition allows the stability analysis to be decoupled into structural and dynamical components, just like the usual MSF for pairwise interactions. However, such powerful reduction comes at an inevitable cost: simplifying assumptions must be made about the network structure (e.g., all-to-all coupling), node dynamics (e.g., fixed points), and/or interaction functions (e.g., linear) in order for the aggregation to a single matrix to be valid.

Here, we consider general oscillators coupled on hypergraphs without the aforementioned restrictions. For the ease of presentation and without loss of generality, we focus on networks with interactions that involve up to three oscillators simultaneously:

$$\begin{aligned} \mathbf{x}_i[t+1] = & \mathbf{F}(\mathbf{x}_i[t]) + \sigma_1 \sum_{j=1}^N A_{ij}^{(1)} \mathbf{H}^{(1)}(\mathbf{x}_i[t], \mathbf{x}_j[t]) \\ & + \sigma_2 \sum_{j=1}^N \sum_{k=1}^N A_{ijk}^{(2)} \mathbf{H}^{(2)}(\mathbf{x}_i[t], \mathbf{x}_j[t], \mathbf{x}_k[t]). \end{aligned} \quad (5)$$

The adjacency matrix $\mathbf{A}^{(1)}$ and adjacency tensor $\mathbf{A}^{(2)}$ represent the pairwise and the three-body interaction, respectively. To make progress, we use the following key insight from Ref. [47]: for noninvasive coupling [i.e., $\mathbf{H}^{(1)}(\mathbf{s}, \mathbf{s}) = 0$ and $\mathbf{H}^{(2)}(\mathbf{s}, \mathbf{s}, \mathbf{s}) = 0$] and global synchronization, synchronization stability in hypergraphs is determined by Eq. (4) with $\mathbf{C}^{(k)} = -\mathbf{L}^{(k)}$, where $\mathbf{L}^{(k)}$ are generalized Laplacians defined based on the adjacency tensors $\mathbf{A}^{(k)}$. More concretely, $\mathbf{L}^{(1)}$ is the usual Laplacian, for which $L_{ij}^{(1)} = \delta_{ij} \sum_k A_{ik}^{(1)} - A_{ij}^{(1)}$; $\mathbf{L}^{(2)}$ retains the zero row-sum property and is defined as $L_{ij}^{(2)} = -\sum_k A_{ijk}^{(2)}$ for $i \neq j$ and $L_{ii}^{(2)} = -\sum_{k \neq i} L_{ik}^{(2)}$. Higher-order generalized Laplacians for $k > 2$ can be defined similarly.

Crucially, we can show that the generalized Laplacians are sufficient for the stability analysis of *cluster* synchro-

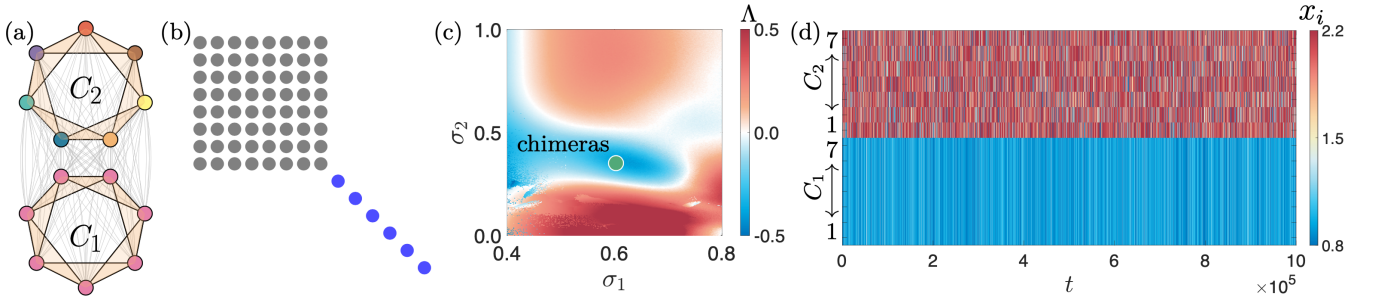


FIG. 1. Chimera states arising from nonpairwise interactions. (a) Two identical clusters of optoelectronic oscillators. The three-body interactions are indicated by 2-simplices (beige triangles). The eight dynamical clusters that form the chimera state are indicated by different colors. (b) Common block structure of the matrices in the variational equation [Eq. (4)] revealed by the SBD algorithm. (c) Linear stability analysis of chimera states based on the SBD coordinates for a range of pairwise interaction strength σ_1 and three-body interaction strength σ_2 . Chimeras are stable when the maximum transverse Lyapunov exponent Λ is negative. (d) Chimera dynamics for $\sigma_1 = 0.6$ and $\sigma_2 = 0.4$ [green dot in (c)].

nization patterns provided that the clusters are nonintertwined [48, 49] (see Supplemental Material for details [18]). Thus, in these cases, the problem reduces to applying the SBD algorithm to the set formed by matrices $\{\mathbf{D}^{(m)}\}$ (determined by the synchronization pattern) and $\{\mathbf{L}^{(k)}\}$ (encoding the hypergraph structure). The resulting SBD coordinates automatically separate the perturbations transverse to the cluster synchronization manifold from the ones parallel to the manifold. The transverse perturbations dictate the stability of the cluster synchronization state and are optimally decoupled under the SBD coordinates. This significantly simplifies the calculation of Lyapunov exponents in Eq. (4) and can provide valuable insight on the origin of instability.

As an application to nontrivial synchronization patterns, we study chimera states [50, 51] on hypergraphs. The hypergraph in Fig. 1(a) consists of two clusters of optoelectronic oscillators. Each cluster is a simplicial complex, in which a node is coupled to its four nearest neighbors through pairwise interactions of strength σ_1 and it also participates in three-body interactions of strength σ_2 . The two clusters are all-to-all coupled through weaker links of strength $\kappa\sigma_1$, and in our simulations we take $\kappa = 1/5$. The individual oscillators are modeled as discrete maps $x_i[t+1] = \beta \sin^2(x_i[t] + \pi/4)$, where β is the self-feedback strength that is tunable in experiments [52]. For the pairwise interaction, we set $H^{(1)}(x_i, x_j) = \sin^2(x_j + \pi/4) - \sin^2(x_i + \pi/4)$. For the three-body interaction, we set $H^{(2)}(x_i, x_j, x_k) = \sin^2(x_j + x_k - 2x_i)$.

To characterize chimera states for which one cluster is synchronized and one cluster is incoherent, we are confronted with 10 noncommuting matrices in Eq. (4). Eight of them are $\{\mathbf{D}^{(1)}, \dots, \mathbf{D}^{(8)}\}$ corresponding to one dynamical cluster with 7 synchronized nodes and seven dynamical clusters with 1 node each [distinguished by colors in Fig. 1(a)]. The other two matrices are $\{\mathbf{L}^{(1)}, \mathbf{L}^{(2)}\}$, which describe the pairwise and three-body interactions, respectively. Applying the SBD algorithm to these ma-

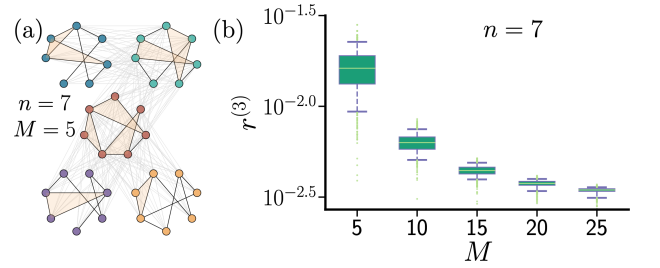


FIG. 2. Reducing the complexity of analyzing synchronization patterns in hypergraphs. (a) Example hypergraph consisting of $M = 5$ clusters, each with $n = 7$ nodes. (b) Reduction in computational complexity achieved by the SBD algorithm for $n = 7$, $p = 0.5$, and $q = 0.5$ as M is varied. The box covers the range 25th–75th percentile, the whiskers mark the range 5th–95th percentile, and the dots indicate the remaining 10% outliers. Each boxplot is based on 1000 independent network realizations.

trices reveals the common block structure depicted in Fig. 1(b). The gray block corresponds to perturbations parallel to the cluster synchronization manifold and doesn't affect the chimera stability. The blue blocks control the transverse perturbations and are included in the stability analysis. This allows us to focus on one 1×1 block at a time and to efficiently calculate the maximum transverse Lyapunov exponent (MTLE) Λ of the chimera state using previously established procedure for chimera stability analysis [53]. In particular, we can calculate the MTLE in the σ_1 - σ_2 parameter space to map out the stable chimera region. As can be seen from Fig. 1(c), where we fix $\beta = 1.5$, chimera states are unstable when oscillators are coupled only through pairwise interactions (i.e., when $\sigma_2 = 0$), but they become stable in the presence of three-body interactions of intermediate strength. Figure 1(d) shows the typical chimera dynamics for $\beta = 1.5$, $\sigma_1 = 0.6$, and $\sigma_2 = 0.4$.

To test the SBD algorithm systematically, we consider networks consisting of M dynamical clusters, each with

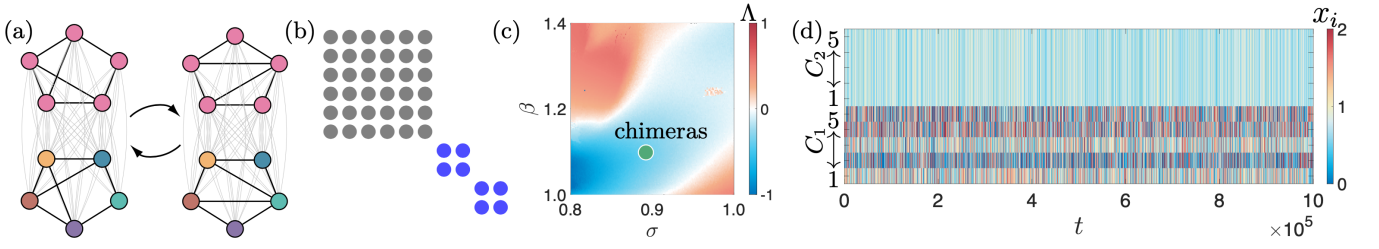


FIG. 3. Chimera states on a temporal network, whose intracluster connections alternate between two configurations. The panels are the equivalents of the ones in Fig. 1.

n nodes [Fig. 2(a)], such that: 1) each cluster is a random subnetwork with link density p , to which three-body interactions are added by transforming triangles into 2-simplices; 2) two clusters are either all-to-all connected (with probability $q > 0$) or fully disconnected from each other (with probability $1 - q$). In the analysis of the M -cluster synchronization state in these networks, the reduction in computational complexity yielded by the SBD algorithm can be measured using $r^{(\alpha)} = \sum_i n_i^\alpha / N^\alpha$, where n_i is the size of the i th common block for the transformed matrices. If the computational complexity of analyzing Eq. (4) in its original form scales as $\mathcal{O}(N^\alpha)$, then $r^{(\alpha)}$ gives the fraction of time needed to analyze Eq. (4) in its decoupled form under the SBD coordinates. Given that the computational complexity of finding the Lyapunov exponents for a fixed point in an n_i -dimensional space typically lies between $\mathcal{O}(n_i^2)$ and $\mathcal{O}(n_i^3)$, here we set $\alpha = 3$ as a reference for the more challenging task of calculating the Lyapunov exponents for periodic or chaotic trajectories.

In Fig. 2(b), we apply the SBD algorithm to $\{\mathbf{D}^{(1)}, \dots, \mathbf{D}^{(M)}, \mathbf{L}^{(1)}, \mathbf{L}^{(2)}\}$ and plot $r^{(3)}$ against the number of clusters M in the networks. We see a reduction in complexity of at least two orders of magnitude ($r^{(3)} \leq 10^{-2}$) for $M \geq 10$. This reduction does not depend sensitively on other parameters in our model (n , p , and q).

Multilayer and temporal networks.— The coexistence of different types (i.e., layers) of interactions in a network [4, 5, 54] can dramatically influence underlying dynamical processes, such as diffusion [55, 56] and synchronization [57, 58]. Multilayer networks of N oscillators diffusively coupled through K different types of interactions can be described by

$$\mathbf{x}_i[t+1] = \mathbf{F}(\mathbf{x}_i[t]) - \sum_{k=1}^K \sigma_k \sum_{j=1}^N L_{ij}^{(k)} \mathbf{H}^{(k)}(\mathbf{x}_j[t]), \quad (6)$$

where $\mathbf{L}^{(k)}$ is the Laplacian matrix representing the links mediating interactions of the form $\mathbf{H}^{(k)}$ and coupling strength σ_k . It is easy to see that the corresponding variational equation for a given synchronization pattern [23, 59] is a special case of Eq. (4) and can be readily addressed using the SBD algorithm.

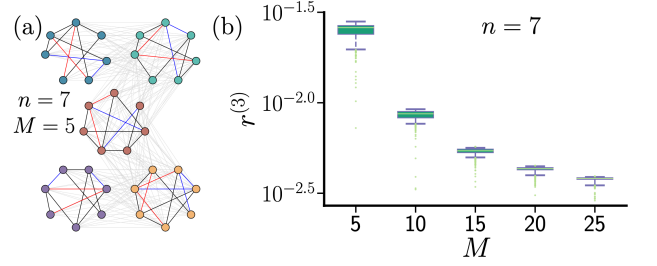


FIG. 4. Equivalent of Fig. 2 for temporal networks. Each temporal network consists of M clusters with time-varying connections. In each cluster, an expected 20% of the links are temporal (connections alternate between the blue and the red lines) and the remaining 80% are static (black lines).

Another class of systems that lend themselves naturally to be addressed using our SBD framework are temporal networks [6]. Such networks are ubiquitous in nature and society [60, 61], and their time-varying nature has been shown to significantly alter many dynamical characteristics, including controllability [60] and synchronizability [62, 63].

Consider a temporal network whose connection pattern at time t is described by $\mathbf{L}^{(t)}$,

$$\mathbf{x}_i[t+1] = \mathbf{F}(\mathbf{x}_i[t]) - \sigma \sum_{j=1}^N L_{ij}^{(t)} \mathbf{H}(\mathbf{x}_j[t]). \quad (7)$$

Here, the stability analysis of synchronization patterns can be simplified by simultaneously block diagonalizing $\{\mathbf{D}^{(m)}\}$ and $\{\mathbf{L}^{(t)}\}$. This framework generalizes the one developed in Ref. [64], which assumes that synchronization is global and the set of all $\mathbf{L}^{(t)}$ to be commutative. We also do not require separation of time scales between the evolution of the network structure and the internal dynamics of oscillators (e.g., the fast switching limit), which was assumed in various blinking models in exchange of analytical insight [65, 66].

As an application, we characterize chimera states on temporal networks that alternate between two different configurations. Figure 3(a) illustrates the temporal evolution of one such network, which has intracluster coupling of strength σ and intercluster coupling of strength $\kappa\sigma$ (again for $\kappa = 1/5$ and the same optoelectronic oscillator and pairwise interaction function as in Fig. 1).

This system has a variational equation with noncommuting matrices $\{\mathbf{D}^{(1)}, \dots, \mathbf{D}^{(6)}, \mathbf{L}^{(1)}, \mathbf{L}^{(2)}\}$, where $\mathbf{L}^{(1)}$ and $\mathbf{L}^{(2)}$ correspond to the network configuration at odd and even t , respectively. Applying the SBD algorithm reveals one 6×6 “parallel” block and two 2×2 “transverse” blocks [Fig. 3(b)], effectively reducing the dimension of the problem from 10 to 2. The chimera region based on the MTLE calculated under the SBD coordinates is shown in Fig. 3(c) and the typical chimera dynamics for $\sigma = 0.9$ and $\beta = 1.1$ are presented in Fig. 3(d).

To further demonstrate the utility of the SBD framework, we consider more systematically temporal networks that alternate between two different configurations. The network construction is similar to that in Fig. 2, except that here each cluster has time-varying instead of non-pairwise interactions. In the example shown in Fig. 4(a), each cluster has red links active at odd t and blue links active at even t , while the black links are always active. Figure 4(b) confirms that the SBD algorithm consistently leads to substantial reduction in computational complexity. Moreover, as in the case of hypergraphs (Fig. 2), the complexity reduction increases as the number M of clusters increases. Again, the results are largely independent of the cluster size and link densities.

Conclusions.— In this work we established SBD as a versatile tool to analyze complex synchronization patterns in generalized networks with nonpairwise, multilayer, and time-varying interactions. The method can be easily applied to other dynamical processes, such as diffusion [56], random walks [35], and consensus [67]. Indeed, the equations describing such processes on generalized networks often involve two or more noncommuting matrices, whose SBD naturally leads to an optimal mode decoupling and the simplification of the analysis. Our SBD algorithm is highly scalable, with a computational complexity of $\mathcal{O}(N^3)$ that is dominated by the cost of finding the eigenvectors of an $N \times N$ symmetric matrix. The computational time used to find SBD coordinates is thus negligible compared with the time needed to perform the stability analysis (i.e., the calculation of the Lyapunov exponents). This is especially true for chaotic oscillators, for which the variational equation needs to be integrated over the entire chaotic attractor. Moreover, given a network and a synchronization pattern, the transformation needs to be calculated only once since the same SBD coordinates can be reused for different choices of parameters (as in our parameter space characterization of the stability of chimera states). We thus expect that the SBD framework will facilitate the exploration of collective dynamics beyond traditional networks.

The authors thank Fiona Brady, Anastasiya Salova, and Raissa D’Souza for insightful discussions. This work was supported by ARO Grant No. W911NF-19-1-0383. Y.Z. also acknowledges support from the Schmidt Science Fellowship. V.L. was funded by the Leverhulme Trust Research Fellowship “CREATE: The Network Compo-

nents of Creativity and Success.”

-
- [1] S. H. Strogatz, Exploring complex networks, *Nature* **410**, 268 (2001).
 - [2] M. E. Newman, The structure and function of complex networks, *SIAM Rev.* **45**, 167 (2003).
 - [3] F. Battiston, G. Cencetti, I. Iacopini, V. Latora, M. Lucas, A. Patania, J.-G. Young, and G. Petri, Networks beyond pairwise interactions: Structure and dynamics, *Phys. Rep.* **874**, 1 (2020).
 - [4] M. Kivelä, A. Arenas, M. Barthelemy, J. P. Gleeson, Y. Moreno, and M. A. Porter, Multilayer networks, *J. Complex Netw.* **2**, 203 (2014).
 - [5] S. Boccaletti, G. Bianconi, R. Criado, C. I. Del Genio, J. Gómez-Gardenes, M. Romance, I. Sendina-Nadal, Z. Wang, and M. Zanin, The structure and dynamics of multilayer networks, *Phys. Rep.* **544**, 1 (2014).
 - [6] P. Holme and J. Saramäki, Temporal networks, *Phys. Rep.* **519**, 97 (2012).
 - [7] I. Stewart, M. Golubitsky, and M. Pivato, Symmetry groupoids and patterns of synchrony in coupled cell networks, *SIAM J. Appl. Dyn. Syst.* **2**, 609 (2003).
 - [8] V. N. Belykh, G. V. Osipov, V. S. Petrov, J. A. Suykens, and J. Vandewalle, Cluster synchronization in oscillatory networks, *Chaos* **18**, 037106 (2008).
 - [9] T. Dahms, J. Lehnert, and E. Schöll, Cluster and group synchronization in delay-coupled networks, *Phys. Rev. E* **86**, 016202 (2012).
 - [10] V. Nicosia, M. Valencia, M. Chavez, A. Díaz-Guilera, and V. Latora, Remote synchronization reveals network symmetries and functional modules, *Phys. Rev. Lett.* **110**, 174102 (2013).
 - [11] C. R. Williams, T. E. Murphy, R. Roy, F. Sorrentino, T. Dahms, and E. Schöll, Experimental observations of group synchrony in a system of chaotic optoelectronic oscillators, *Phys. Rev. Lett.* **110**, 064104 (2013).
 - [12] D. P. Rosin, D. Rontani, D. J. Gauthier, and E. Schöll, Control of synchronization patterns in neural-like boolean networks, *Phys. Rev. Lett.* **110**, 104102 (2013).
 - [13] C. Fu, Z. Deng, L. Huang, and X. Wang, Topological control of synchronous patterns in systems of networked chaotic oscillators, *Phys. Rev. E* **87**, 032909 (2013).
 - [14] A. Schnitzler and J. Gross, Normal and pathological oscillatory communication in the brain, *Nat. Rev. Neurosci.* **6**, 285 (2005).
 - [15] F. Blaabjerg, R. Teodorescu, M. Liserre, and A. V. Timbus, Overview of control and grid synchronization for distributed power generation systems, *IEEE Trans. Ind. Electron.* **53**, 1398 (2006).
 - [16] R. M. Reinhart and J. A. Nguyen, Working memory revived in older adults by synchronizing rhythmic brain circuits, *Nat. Neurosci.* **22**, 820 (2019).
 - [17] L. M. Pecora and T. L. Carroll, Master stability functions for synchronized coupled systems, *Phys. Rev. Lett.* **80**, 2109 (1998).
 - [18] See Supplemental Material for a proof of the optimality of the block structure given by the SBD algorithm and the variational equation for nonintertwined clusters in hypergraphs.

- [19] T. Maehara and K. Murota, A numerical algorithm for block-diagonal decomposition of matrix \ast -algebras with general irreducible components, *Jpn. J. Ind. Appl. Math* **27**, 263 (2010).
- [20] T. Maehara and K. Murota, Algorithm for error-controlled simultaneous block-diagonalization of matrices, *SIAM J. Matrix Anal. Appl.* **32**, 605 (2011).
- [21] D. Irving and F. Sorrentino, Synchronization of dynamical hypernetworks: Dimensionality reduction through simultaneous block-diagonalization of matrices, *Phys. Rev. E* **86**, 056102 (2012).
- [22] Y. Zhang and A. E. Motter, Identical synchronization of nonidentical oscillators: When only birds of different feathers flock together, *Nonlinearity* **31**, R1 (2018).
- [23] Y. Zhang and A. E. Motter, Symmetry-independent stability analysis of synchronization patterns, *arXiv:2003.05461* (2020).
- [24] <https://github.com/y-z-zhang/SBD>.
- [25] C. Berge, *Graphs and hypergraphs* (North-Holland, 1973).
- [26] A. Hatcher, *Algebraic topology* (Cambridge University Press, 2002).
- [27] A. R. Benson, D. F. Gleich, and J. Leskovec, Higher-order organization of complex networks, *Science* **353**, 163 (2016).
- [28] A. R. Benson, R. Abebe, M. T. Schaub, A. Jadbabaie, and J. Kleinberg, Simplicial closure and higher-order link prediction, *Proc. Natl. Acad. Sci. U.S.A.* **115**, E11221 (2018).
- [29] G. Petri and A. Barrat, Simplicial activity driven model, *Phys. Rev. Lett.* **121**, 228301 (2018).
- [30] I. Iacopini, G. Petri, A. Barrat, and V. Latora, Simplicial models of social contagion, *Nat. Commun.* **10**, 2485 (2019).
- [31] M. H. Matheny, J. Emenheiser, W. Fon, A. Chapman, A. Salova, M. Rohden, J. Li, M. H. de Badyn, M. Pósfai, L. Duenas-Osorio, *et al.*, Exotic states in a simple network of nanoelectromechanical oscillators, *Science* **363**, eaav7932 (2019).
- [32] J. T. Matamalas, S. Gómez, and A. Arenas, Abrupt phase transition of epidemic spreading in simplicial complexes, *Phys. Rev. Res.* **2**, 012049 (2020).
- [33] G. F. de Arruda, G. Petri, and Y. Moreno, Social contagion models on hypergraphs, *Phys. Rev. Res.* **2**, 023032 (2020).
- [34] G. St-Onge, V. Thibeault, A. Allard, L. J. Dubé, and L. Hébert-Dufresne, Master equation analysis of mesoscopic localization in contagion dynamics on higher-order networks, *arXiv:2004.10203* (2020).
- [35] M. T. Schaub, A. R. Benson, P. Horn, G. Lippner, and A. Jadbabaie, Random walks on simplicial complexes and the normalized Hodge 1-Laplacian, *SIAM Rev.* **62**, 353 (2020).
- [36] T. Carletti, F. Battiston, G. Cencetti, and D. Fanelli, Random walks on hypergraphs, *Phys. Rev. E* **101**, 022308 (2020).
- [37] T. Tanaka and T. Aoyagi, Multistable attractors in a network of phase oscillators with three-body interactions, *Phys. Rev. Lett.* **106**, 224101 (2011).
- [38] C. Bick, P. Ashwin, and A. Rodrigues, Chaos in generically coupled phase oscillator networks with nonpairwise interactions, *Chaos* **26**, 094814 (2016).
- [39] P. S. Skardal and A. Arenas, Abrupt desynchronization and extensive multistability in globally coupled oscillator simplexes, *Phys. Rev. Lett.* **122**, 248301 (2019).
- [40] P. S. Skardal and A. Arenas, Higher-order interactions in complex networks of phase oscillators promote abrupt synchronization switching, *arXiv:1909.08057* (2019).
- [41] C. Xu, X. Wang, and P. S. Skardal, Bifurcation analysis and structural stability of simplicial oscillator populations, *Phys. Rev. Res.* **2**, 023281 (2020).
- [42] A. P. Millán, J. J. Torres, and G. Bianconi, Explosive higher-order Kuramoto dynamics on simplicial complexes, *Phys. Rev. Lett.* **124**, 218301 (2020).
- [43] R. Mulas, C. Kuehn, and J. Jost, Coupled dynamics on hypergraphs: Master stability of steady states and synchronization, *arXiv:2003.13775* (2020).
- [44] M. Lucas, G. Cencetti, and F. Battiston, Multiorde Laplacian for synchronization in higher-order networks, *Phys. Rev. Res.* **2**, 033410 (2020).
- [45] T. Carletti, D. Fanelli, and S. Nicoletti, Dynamical systems on hypergraphs, *arXiv:2006.01243* (2020).
- [46] G. F. de Arruda, M. Tizzani, and Y. Moreno, Phase transitions and stability of dynamical processes on hypergraphs, *arXiv:2005.10891* (2020).
- [47] L. Gambuzza, F. Di Patti, L. Gallo, S. Lepri, M. Romance, R. Criado, M. Frasca, V. Latora, and S. Boccaletti, The master stability function for synchronization in simplicial complexes, *arXiv:2004.03913* (2020).
- [48] L. M. Pecora, F. Sorrentino, A. M. Hagerstrom, T. E. Murphy, and R. Roy, Cluster synchronization and isolated desynchronization in complex networks with symmetries, *Nat. Commun.* **5**, 4079 (2014).
- [49] Y. S. Cho, T. Nishikawa, and A. E. Motter, Stable chimeras and independently synchronizable clusters, *Phys. Rev. Lett.* **119**, 084101 (2017).
- [50] M. J. Panaggio and D. M. Abrams, Chimera states: Coexistence of coherence and incoherence in networks of coupled oscillators, *Nonlinearity* **28**, R67 (2015).
- [51] O. E. Omel'chenko, The mathematics behind chimera states, *Nonlinearity* **31**, R121 (2018).
- [52] J. D. Hart, D. C. Schmadel, T. E. Murphy, and R. Roy, Experiments with arbitrary networks in time-multiplexed delay systems, *Chaos* **27**, 121103 (2017).
- [53] Y. Zhang, Z. G. Nicolaou, J. D. Hart, R. Roy, and A. E. Motter, Critical switching in globally attractive chimeras, *Phys. Rev. X* **10**, 011044 (2020).
- [54] A. Aleta and Y. Moreno, Multilayer networks in a nutshell, *Annu. Rev. Condens. Matter Phys.* **10**, 45 (2019).
- [55] S. Gomez, A. Díaz-Guilera, J. Gomez-Gardeñes, C. J. Perez-Vicente, Y. Moreno, and A. Arenas, Diffusion dynamics on multiplex networks, *Phys. Rev. Lett.* **110**, 028701 (2013).
- [56] M. De Domenico, C. Granell, M. A. Porter, and A. Arenas, The physics of spreading processes in multilayer networks, *Nat. Phys.* **12**, 901 (2016).
- [57] V. Nicosia, P. S. Skardal, A. Arenas, and V. Latora, Collective phenomena emerging from the interactions between dynamical processes in multiplex networks, *Phys. Rev. Lett.* **118**, 138302 (2017).
- [58] I. Belykh, D. Carter, and R. Jeter, Synchronization in multilayer networks: when good links go bad, *SIAM J. Appl. Dyn. Syst.* **18**, 2267 (2019).
- [59] F. Della Rossa, L. M. Pecora, K. Blaha, A. Shirin, I. Klickstein, and F. Sorrentino, Symmetries and cluster synchronization in multilayer networks, *Nat. Commun.* **11**, 3179 (2020).
- [60] A. Li, S. P. Cornelius, Y.-Y. Liu, L. Wang, and A.-L.

- Barabási, The fundamental advantages of temporal networks, *Science* **358**, 1042 (2017).
- [61] A. Paranjape, A. R. Benson, and J. Leskovec, Motifs in temporal networks, in *Proceedings of the Tenth ACM International Conference on Web Search and Data Mining* (2017) pp. 601–610.
- [62] R. Amritkar and C.-K. Hu, Synchronized state of coupled dynamics on time-varying networks, *Chaos* **16**, 015117 (2006).
- [63] R. Jeter and I. Belykh, Synchronization in on-off stochastic networks: windows of opportunity, *IEEE Trans. Circuits Syst. I, Reg. Papers* **62**, 1260 (2015).
- [64] S. Boccaletti, D.-U. Hwang, M. Chavez, A. Amann, J. Kurths, and L. M. Pecora, Synchronization in dynamical networks: Evolution along commutative graphs, *Phys. Rev. E* **74**, 016102 (2006).
- [65] I. V. Belykh, V. N. Belykh, and M. Hasler, Blinking model and synchronization in small-world networks with a time-varying coupling, *Physica D* **195**, 188 (2004).
- [66] D. J. Stilwell, E. M. Bollt, and D. G. Roberson, Sufficient conditions for fast switching synchronization in time-varying network topologies, *SIAM J. Appl. Dyn. Syst.* **5**, 140 (2006).
- [67] L. Neuhäuser, A. Mellor, and R. Lambiotte, Multibody interactions and nonlinear consensus dynamics on networked systems, *Phys. Rev. E* **101**, 032310 (2020).

SUPPLEMENTAL MATERIAL

Unified Treatment of Dynamical Processes on Generalized Networks: Higher-Order, Multilayer, and Temporal Interactions

Yuanzhao Zhang, Vito Latora, and Adilson E. Motter

I. OPTIMALITY OF THE COMMON BLOCK STRUCTURE DISCOVERED BY THE SBD ALGORITHM

Given a set of symmetric matrices $\mathcal{B} = \{\mathbf{B}^{(1)}, \mathbf{B}^{(2)}, \dots, \mathbf{B}^{(\mathcal{L})}\}$, let $\mathbf{B} = \sum_{\ell=1}^{\mathcal{L}} \xi_{\ell} \mathbf{B}^{(\ell)}$, where ξ_{ℓ} are random coefficients. Without loss of generality, we can assume all matrices $\mathbf{B}^{(\ell)}$ to be in their finest common block form. Our goal is then to prove that, with probability 1, each eigenvector \mathbf{v}_i of \mathbf{B} is “localized” within a single (square) block, meaning that the indices of the nonzero entries of \mathbf{v}_i are limited to the rows of one of the common blocks shared by $\{\mathbf{B}^{(\ell)}\}$ (Fig. S1).

We first notice that \mathbf{B} inherits the common block structure of $\{\mathbf{B}^{(\ell)}\}$. Thus, for each $n_i \times n_i$ block shared by $\{\mathbf{B}^{(\ell)}\}$, we can always find n_i eigenvectors of \mathbf{B} that are “localized” within that block. When the eigenvalues of \mathbf{B} are nondegenerate, the eigenvectors are unique, and thus all $N = \sum_i n_i$ eigenvectors of matrix \mathbf{B} are localized within individual blocks.

If the matrix \mathbf{B} includes eigenvectors with degenerate eigenvalues, then this is either caused by a non-generic choice of $\{\xi_{\ell}\}$ or by all matrices $\mathbf{B}^{(\ell)}$ sharing the same set of degenerate eigenvectors. The first scenario does not persist upon infinitesimal variation in ξ_{ℓ} and thus occurs with probability 0. The second scenario implies that all matrices $\mathbf{B}^{(\ell)}$ are simultaneously diagonalized in the subspace spanned by these eigenvectors, corresponding to 1×1 blocks in their finest common block form. We have assumed that the matrices $\mathbf{B}^{(\ell)}$ are in this form. Thus, even when \mathbf{B} has degenerate eigenvectors (which we choose to be orthogonal to each other), all the eigenvectors still match the common block structure shared by $\{\mathbf{B}^{(\ell)}\}$ with probability 1.

Based on the results above, it follows that after computing the eigenvectors \mathbf{v}_i of matrix \mathbf{B} (step *i* of the SBD algorithm) and sorting them according to their associated block (steps *ii* and *iii* of the SBD algorithm), the resulting orthogonal matrix $\mathbf{P} = [\mathbf{v}_{\epsilon(1)}, \dots, \mathbf{v}_{\epsilon(N)}]$ will, with probability 1, reveal the finest common block structure. Here, “finest” is characterized by the number of common blocks being maximal (which is also equivalent to the sizes of the blocks being minimal), and the block sizes are unique up to permutations.

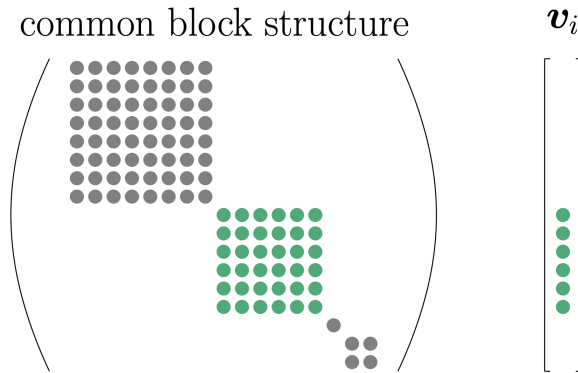


Figure S1. Illustration of an eigenvector \mathbf{v}_i that is “localized” within the green block. Nonzero entries are represented as solid circles.

II. VARIATIONAL EQUATION FOR NONINTERTWINED CLUSTERS IN HYPERGRAPHS

The variational equation for a cluster synchronization pattern on a hypergraph has the following form:

$$\begin{aligned}
\delta_i[t+1] = & \mathbf{J}\mathbf{F}(\mathbf{s}^{m(i)}[t])\delta_i[t] + \sigma_1 \sum_j A_{ij}^{(1)} (\partial_{\mathbf{x}_i} \mathbf{H}^{(1)}(\mathbf{x}_i, \mathbf{x}_j) |_{(\mathbf{s}^{m(i)}, \mathbf{s}^{m(j)})}) \delta_i[t] + \partial_{\mathbf{x}_j} \mathbf{H}^{(1)}(\mathbf{x}_i, \mathbf{x}_j) |_{(\mathbf{s}^{m(i)}, \mathbf{s}^{m(j)})} \delta_j[t] \\
& + \sigma_2 \sum_{j,k} A_{ijk}^{(2)} (\partial_{\mathbf{x}_i} \mathbf{H}^{(2)}(\mathbf{x}_i, \mathbf{x}_j, \mathbf{x}_k) |_{(\mathbf{s}^{m(i)}, \mathbf{s}^{m(j)}, \mathbf{s}^{m(k)})}) \delta_i[t] + \partial_{\mathbf{x}_j} \mathbf{H}^{(2)}(\mathbf{x}_i, \mathbf{x}_j, \mathbf{x}_k) |_{(\mathbf{s}^{m(i)}, \mathbf{s}^{m(j)}, \mathbf{s}^{m(k)})} \delta_j[t] + \\
& \partial_{\mathbf{x}_k} \mathbf{H}^{(2)}(\mathbf{x}_i, \mathbf{x}_j, \mathbf{x}_k) |_{(\mathbf{s}^{m(i)}, \mathbf{s}^{m(j)}, \mathbf{s}^{m(k)})} \delta_k[t] + \sigma_3 \sum_{j,k,\ell} A_{ijk\ell}^{(3)} \cdots, \quad i = 1, 2, \dots, N,
\end{aligned} \tag{S1}$$

where $m(i)$ denotes the cluster to which node i belongs.

Since the clusters are not intertwined, each oscillator in the same cluster is affected by perturbations in other clusters in the same way [1, 2]. Thus, for all nodes i that belong to a cluster m , the terms from Eq. (S1) involving δ_j for $j \notin m$ can be combined into a single aggregated term \mathbf{I}_m . Moreover, each oscillator in cluster m receives the same number of links $\mu_{m' \rightarrow m}$ from a different cluster m' . Using these conditions, the σ_1 term from Eq. (S1), which arise from the pairwise interactions, can be simplified to

$$\begin{aligned}
& \sum_j A_{ij}^{(1)} (\partial_{\mathbf{x}_i} \mathbf{H}^{(1)}(\mathbf{x}_i, \mathbf{x}_j) |_{(\mathbf{s}^{m(i)}, \mathbf{s}^{m(j)})}) \delta_i[t] + \partial_{\mathbf{x}_j} \mathbf{H}^{(1)}(\mathbf{x}_i, \mathbf{x}_j) |_{(\mathbf{s}^{m(i)}, \mathbf{s}^{m(j)})} \delta_j[t] \\
= & \sum_{j \in m(i)} A_{ij}^{(1)} (\partial_{\mathbf{x}_i} \mathbf{H}^{(1)}(\mathbf{x}_i, \mathbf{x}_j) |_{(\mathbf{s}^{m(i)}, \mathbf{s}^{m(i)})}) \delta_i[t] + \partial_{\mathbf{x}_j} \mathbf{H}^{(1)}(\mathbf{x}_i, \mathbf{x}_j) |_{(\mathbf{s}^{m(i)}, \mathbf{s}^{m(i)})} \delta_j[t] + \\
& \sum_{j \notin m(i)} A_{ij}^{(1)} (\partial_{\mathbf{x}_i} \mathbf{H}^{(1)}(\mathbf{x}_i, \mathbf{x}_j) |_{(\mathbf{s}^{m(i)}, \mathbf{s}^{m(j)})}) \delta_i[t] + \partial_{\mathbf{x}_j} \mathbf{H}^{(1)}(\mathbf{x}_i, \mathbf{x}_j) |_{(\mathbf{s}^{m(i)}, \mathbf{s}^{m(j)})} \delta_j[t] \\
= & \sum_{j \in m(i)} A_{ij}^{(1)} (\partial_{\mathbf{x}_i} \mathbf{H}^{(1)}(\mathbf{x}_i, \mathbf{x}_j) |_{(\mathbf{s}^{m(i)}, \mathbf{s}^{m(i)})}) \delta_i[t] + \partial_{\mathbf{x}_j} \mathbf{H}^{(1)}(\mathbf{x}_i, \mathbf{x}_j) |_{(\mathbf{s}^{m(i)}, \mathbf{s}^{m(i)})} \delta_j[t] + \\
& \sum_{m' \neq m(i)} \mu_{m' \rightarrow m(i)} \partial_{\mathbf{x}_i} \mathbf{H}^{(1)}(\mathbf{x}_i, \mathbf{x}_j) |_{(\mathbf{s}^{m(i)}, \mathbf{s}^{m'})} \delta_i[t] + \mathbf{I}_{m(i)}^{(1)}[t].
\end{aligned} \tag{S2}$$

Since $\mathbf{H}^{(1)}(\mathbf{s}, \mathbf{s}) = 0$ implies $\partial_{\mathbf{x}_i} \mathbf{H}^{(1)}(\mathbf{x}_i, \mathbf{x}_j) |_{(\mathbf{s}, \mathbf{s})} = -\partial_{\mathbf{x}_j} \mathbf{H}^{(1)}(\mathbf{x}_i, \mathbf{x}_j) |_{(\mathbf{s}, \mathbf{s})}$, it follows that the first r.h.s. term in this equation can be expressed using the generalized Laplacian $\mathbf{L}^{(1)}$ as

$$- \sum_{j \in m(i)} L_{ij}^{(1)} \partial_{\mathbf{x}_j} \mathbf{H}^{(1)}(\mathbf{x}_i, \mathbf{x}_j) |_{(\mathbf{s}^{m(i)}, \mathbf{s}^{m(i)})} \delta_j[t], \tag{S3}$$

where the diagonal entries in the generalized Laplacian only count the number of intracluster connections. The second and the third r.h.s. terms can be expressed using the diagonal matrices $\mathbf{D}^{(m)}$, since they both are equal for all nodes within a cluster.

Similarly, for three-body interactions, the corresponding term from Eq. (S1) can be simplified as follows:

$$\begin{aligned}
& \sum_{j,k} A_{ijk}^{(2)} (\partial_{\mathbf{x}_i} \mathbf{H}^{(2)} (\mathbf{x}_i, \mathbf{x}_j, \mathbf{x}_k) |_{(\mathbf{s}^{m(i)}, \mathbf{s}^{m(j)}, \mathbf{s}^{m(k)})} \delta_i[t] + \partial_{\mathbf{x}_j} \mathbf{H}^{(2)} (\mathbf{x}_i, \mathbf{x}_j, \mathbf{x}_k) |_{(\mathbf{s}^{m(i)}, \mathbf{s}^{m(j)}, \mathbf{s}^{m(k)})} \delta_j[t] + \\
& \partial_{\mathbf{x}_k} \mathbf{H}^{(2)} (\mathbf{x}_i, \mathbf{x}_j, \mathbf{x}_k) |_{(\mathbf{s}^{m(i)}, \mathbf{s}^{m(j)}, \mathbf{s}^{m(k)})} \delta_k[t]) \\
&= \sum_{j \in m(i), k \in m(i)} A_{ijk}^{(2)} (\partial_{\mathbf{x}_i} \mathbf{H}^{(2)} (\mathbf{x}_i, \mathbf{x}_j, \mathbf{x}_k) |_{(\mathbf{s}^{m(i)}, \mathbf{s}^{m(i)}, \mathbf{s}^{m(i)})} \delta_i[t] + \partial_{\mathbf{x}_j} \mathbf{H}^{(2)} (\mathbf{x}_i, \mathbf{x}_j, \mathbf{x}_k) |_{(\mathbf{s}^{m(i)}, \mathbf{s}^{m(i)}, \mathbf{s}^{m(i)})} \delta_j[t] + \\
& \partial_{\mathbf{x}_k} \mathbf{H}^{(2)} (\mathbf{x}_i, \mathbf{x}_j, \mathbf{x}_k) |_{(\mathbf{s}^{m(i)}, \mathbf{s}^{m(i)}, \mathbf{s}^{m(i)})} \delta_k[t]) + \\
& \sum_{j \notin m(i), k \notin m(i)} A_{ijk}^{(2)} (\partial_{\mathbf{x}_i} \mathbf{H}^{(2)} (\mathbf{x}_i, \mathbf{x}_j, \mathbf{x}_k) |_{(\mathbf{s}^{m(i)}, \mathbf{s}^{m(j)}, \mathbf{s}^{m(k)})} \delta_i[t] + \partial_{\mathbf{x}_j} \mathbf{H}^{(2)} (\mathbf{x}_i, \mathbf{x}_j, \mathbf{x}_k) |_{(\mathbf{s}^{m(i)}, \mathbf{s}^{m(j)}, \mathbf{s}^{m(k)})} \delta_j[t] + \\
& \partial_{\mathbf{x}_k} \mathbf{H}^{(2)} (\mathbf{x}_i, \mathbf{x}_j, \mathbf{x}_k) |_{(\mathbf{s}^{m(i)}, \mathbf{s}^{m(j)}, \mathbf{s}^{m(k)})} \delta_k[t]) \tag{S4} \\
&= \sum_{j \in m(i), k \in m(i)} A_{ijk}^{(2)} (\partial_{\mathbf{x}_i} \mathbf{H}^{(2)} (\mathbf{x}_i, \mathbf{x}_j, \mathbf{x}_k) |_{(\mathbf{s}^{m(i)}, \mathbf{s}^{m(i)}, \mathbf{s}^{m(i)})} \delta_i[t] + \partial_{\mathbf{x}_j} \mathbf{H}^{(2)} (\mathbf{x}_i, \mathbf{x}_j, \mathbf{x}_k) |_{(\mathbf{s}^{m(i)}, \mathbf{s}^{m(i)}, \mathbf{s}^{m(i)})} \delta_j[t] + \\
& \partial_{\mathbf{x}_k} \mathbf{H}^{(2)} (\mathbf{x}_i, \mathbf{x}_j, \mathbf{x}_k) |_{(\mathbf{s}^{m(i)}, \mathbf{s}^{m(i)}, \mathbf{s}^{m(i)})} \delta_k[t]) + \\
& \sum_{m' \neq m(i) | m'' \neq m(i)} \mu_{m'm'' \rightarrow m(i)} \partial_{\mathbf{x}_i} \mathbf{H}^{(2)} (\mathbf{x}_i, \mathbf{x}_j, \mathbf{x}_k) |_{(\mathbf{s}^{m(i)}, \mathbf{s}^{m'}, \mathbf{s}^{m''})} \delta_i[t] + \\
& \sum_{j \in m(i), m' \neq m(i)} \mu_{m'm(i) \rightarrow m(i)} \partial_{\mathbf{x}_j} \mathbf{H}^{(2)} (\mathbf{x}_i, \mathbf{x}_j, \mathbf{x}_k) |_{(\mathbf{s}^{m(i)}, \mathbf{s}^{m(i)}, \mathbf{s}^{m'})} \delta_j[t] + \\
& \sum_{k \in m(i), m' \neq m(i)} \mu_{m'm(i) \rightarrow m(i)} \partial_{\mathbf{x}_k} \mathbf{H}^{(2)} (\mathbf{x}_i, \mathbf{x}_j, \mathbf{x}_k) |_{(\mathbf{s}^{m(i)}, \mathbf{s}^{m'}, \mathbf{s}^{m(i)})} \delta_k[t] + \mathbf{I}_{m(i)}^{(2)}[t].
\end{aligned}$$

Here, the $|$ symbol under \sum denotes the logical OR operator and $\mu_{m'm'' \rightarrow m}$ represents the number of three-body interactions a node in cluster m receives that involve a node from cluster m' and another node from cluster m'' . Again, using the noninvasive property $\mathbf{H}^{(2)}(\mathbf{s}, \mathbf{s}, \mathbf{s}) = 0$, the first r.h.s. term in this equation can be expressed using the generalized Laplacian $\mathbf{L}^{(2)}$ as

$$- \sum_{j \in m(i)} L_{ij}^{(2)} (\partial_{\mathbf{x}_j} \mathbf{H}^{(2)} (\mathbf{x}_i, \mathbf{x}_j, \mathbf{x}_k) |_{(\mathbf{s}^{m(i)}, \mathbf{s}^{m(i)}, \mathbf{s}^{m(i)})} + \partial_{\mathbf{x}_k} \mathbf{H}^{(2)} (\mathbf{x}_i, \mathbf{x}_j, \mathbf{x}_k) |_{(\mathbf{s}^{m(i)}, \mathbf{s}^{m(i)}, \mathbf{s}^{m(i)})}) \delta_j[t], \tag{S5}$$

where the entries in $\mathbf{L}^{(2)}$ only take into account the intracluster 2-simplices [3]. Similarly to the case of pairwise interactions, the other r.h.s. terms can be expressed using the diagonal matrices $\mathbf{D}^{(m)}$. The derivations above can be easily adapted to include higher-order interactions that involve more than three nodes simultaneously.

-
- [1] L. M. Pecora, F. Sorrentino, A. M. Hagerstrom, T. E. Murphy, and R. Roy, Cluster synchronization and isolated desynchronization in complex networks with symmetries, *Nat. Commun.* **5**, 4079 (2014).
 - [2] Y. S. Cho, T. Nishikawa, and A. E. Motter, Stable chimeras and independently synchronizable clusters, *Phys. Rev. Lett.* **119**, 084101 (2017).
 - [3] L. Gambuzza, F. Di Patti, L. Gallo, S. Lepri, M. Romance, R. Criado, M. Frasca, V. Latora, and S. Boccaletti, The master stability function for synchronization in simplicial complexes, *arXiv:2004.03913* (2020).